

Full Length Research Paper

Histological studies of the visual relay centres in cyanide toxicity: Mode of neuronal cell death in the V1, lateral geniculate body (LGB) and superior colliculus (SC) of adult Wistar rats

Ogundele O. M.^{1*}, Enuaike B. U.², Igwe J.³, Olu-Bolaji A. A.⁴ and Caxton-Martins E. A.²

¹Trinitron Biotech LTD, Science and Technology Complex, Sheda, Abuja, Nigeria.

²University of Ilorin, Department of Anatomy, Ilorin. Nigeria.

³National Hospital, Department of Histopathology, Central Area, Abuja, Nigeria.

⁴Department of Epidemiology and Community Health, University of Ilorin, Nigeria.

Accepted 25 August, 2011

Loss of sight has been a major disorder associated with progressive neurodegenerative disorder involving motor and cognitive dysfunction. Currently, there is no effective treatment either for symptomatic relief or disease modification. This relates, in part, to a lack of knowledge of the underlying neurochemical abnormalities, including cholinergic neurons status in the diffused system of the visual relay centres. To determine histologically the possible adopted mode of cell death in the visual relay centres, previous studies have shown difference in cell death based on treatment dosage and location in brain. 50 F1 generation adult Wistar rats were treated with potassium hexacyanoferrate for a period of 30 days and the tissues were processed histologically (Hematoxylin and eosin, Gordon and sweets and crystal violet) to determine the cellular changes and characterize as apoptotic or necrotic. The predominant mode of cell death in the V1 is apoptosis while necrotic tissue sites were found to exist in the superior colliculus (SC) of the same treatment, certain cells in the lateral geniculate body (LGB) showed morphological features of both apoptosis and necrosis.

Key words: Cyanide, toxicity, visual relay centres, cell death, necrosis, apoptosis.

INTRODUCTION

Cyanide as earlier described is a potent neurotoxic substance that can initiate series of intracellular reactions leading to cell dysfunction and eventually cell death; it enhances N-Methyl-D-Aspartate (NMDA) receptor function (de Haro, 2009; de La Cruz et al., 2009). In cultured neurons, cyanide neurotoxicity is linked with NMDA receptors, mediated rise in calcium that in turn activates series of biochemical reactions leading to generation of reactive oxygen species (ROS) and nitric oxide (NO), This anti-oxidants species then mediates peroxidation of lipids (de Haro, 2009; Varone et al., 2008; Almer et al., 2006). It is concluded that oxidative stress plays an important role in cyanide induced neurodegeneration; this phenomena can cause cell death

1. Apoptosis,
2. Necrosis.

in two ways. Depending on the cell type or stimuli, a cell may die in either of the two distinct ways. Apoptosis considers the physiological form of cell death, it is an acute process with distinct morphological and biochemical features (Bathachanya and Lakshimana, 2001; Quintavalle et al., 2010). Apoptotic cells are characterized by condensed and fragmented nuclei where as necrotic cells show less plasma membrane integrity without apparent nuclei damage. This two different forms of cell death can be elicited by the same stimuli depending on the intensity of the effects (Isom et al., 1999), suggesting that an initial common event can be shared by both forms of cell death. It has been shown previously that cyanide induce cell death in a varying mode for different brain areas (Prabhakaran et al., 2007;

*Corresponding author. E-mail: mikealslaw@hotmail.com. Tel: +2347031022702.

Pedro et al., 2010). Cell death occurs predominantly via apoptosis in the cortical region while necrosis was observed in the substantia nigra after the same dose of cyanide was administered in the mice. Selective vulnerability of different aspect of the brain to cyanide may be explained by the triggering of region specific toxic pathways in which oxidative stress may be a common activator (Isom et al., 1999).

In the two modes of cell death, oxidative stress was a factor but the level of ROS generated varies with the cell types, other reports that oxidative stress can be involved in apoptosis or necrosis (BathaCharrya and Tuwalsami, 2008), it is possible that when high ROS accumulated in the cell, direct and irreversible damage to cell components can lead to necrosis. Moderate levels of ROS may function as cellular messengers and regulatory molecule which mediates apoptotic cell death (Li et al., 2000), in mesencephalic cells, cyanide induced a progressive but rather small increase in necrosis at the concentrations of 100 to 300 μM and at 400 μM the data recorded shows a steep rise in necrotic index.

Organisms use physiological cell death for a variety of reasons. We need to know how many different cell death programs there are, whether and when they interact, and their precise molecular nature. In the past, cell death has been identified and studied descriptively. The term "apoptosis" is often used to describe the physiological death of mammalian cells. When individual cells die in a healthy organ, their death is not accompanied by changes that are characteristic of pathological cell deaths. Apoptosis is associated with death of isolated cells, rather than contiguous patches or areas of tissue; there is no inflammatory infiltrate; nuclear shrinkage occurs relatively early, but changes to the organelles and loss of membrane integrity are relatively late; the dying cells are phagocytosed by neighbouring cells, rather than immigrant professional phagocytes; the DNA is rapidly broken down. The degraded DNA from apoptotic cells forms a characteristic ladder when analyzed by electrophoresis because endonucleases gain access to the DNA in the internucleosomal regions (de Haro, 2009; Varone et al., 2008; Almer et al., 2006; Phrabakharan et al., 2007). The same ladder is produced from the DNA of cells killed by cytotoxic T cells (Vicente et al., 2006; Isom et al., 1999). Necrosis, on the other hand, affects many adjoining cells (Gamper et al., 2005; Pedro et al., 2010; Mathangi and Navasayami, 2000). It is characterized by cell swelling, with early loss of plasma-membrane integrity and major nucleus tends to swell. Necrosis is accompanied by inflammatory infiltrate phagocytic cells. DNA degradation, if it occurs, is a late event (Katherine et al., 2001). The term "programmed cell death" is commonly used synonymously with apoptosis. Apoptosis is more of a descriptive term, whereas programmed cell death implies that the decision to die was made by the cell-autonomously, independently of any other cells. Both terms suggest that the cell is an active participant in its own death. Unfortunately, the terms are not clearly defined,

and different investigators have used different criteria in their classification. Evidence that inhibitors of macromolecular synthesis block cell death argue that the cell is, indeed, actively involved in its own demise (Bonfoco et al., 1995), but in just as many cases macromolecular-synthesis inhibitors do not protect cells, so the cell-death machinery presumably already exists (Gilman et al., 2010). To add to the confusion, there are numerous reports of actinomycin D and cycloheximide themselves triggering apoptosis (Sharma and Chalam, 2009; Lee et al., 2010).

Thus, the effect of macromolecular- synthesis inhibitors on cell death is of no help in determining whether it is physiological. The term "programmed cell death" is also problematic. If it is used strictly, referring only to purely cell-autonomous cell deaths, most physiological cell deaths would have to be excluded, as many cell deaths are triggered by other cells, or products of other cells. The term "physiological cell death" indicates that the cell has died by a mechanism that has evolved specifically by the host to kill its own cells and probably includes most of what has been described as "programmed cell death" and "apoptosis." This term also includes cell deaths that may not exhibit some of the typical features of apoptosis, such as DNA degradation. There may be several different mechanisms that carry out physiological cell deaths. Inappropriate activation of these mechanisms, or their inhibition, may then lead to what can be recognized as pathology. The term "physiological cell death," however, distinguishes the death of the host's cells by the host's machinery from those deaths caused by external agents, such as infections, extremes of temperature, toxins, or deprivation of some vital nutrients. Nevertheless, some external agents may trigger inappropriate activation of physiological cell-death mechanisms, such as when radiation causes the interphase death of lymphocytes, or intestinal epithelial cells are exposed to anticancer agents, or when cells are exposed to extremes of temperature (Behar et al., 1999).

MATERIALS AND METHODS

Animal preparation

50 F_1 generation adult male Wistar rats (*Rattus norvegicus*) each weighing on the average 250 g, were bred from parents adult Wistar rats procured from the animal facility of the National institute for pharmaceutical Research and Development, Idu, Abuja (NIPRD). The animals were weaned on 44th day after birth and were divided into five groups of 10 animals each selected at random irrespective of parental origin using the method of Svensden and Hau (1994). The weight of the animals were obtained at an interval of 3 days using a sensitive weighing balance (Jenway).

Treatment solution and mode of administration

A standard isotonic solution of 0.25 M sucrose was prepared to dissolve the potassium hexacyanoferrate III, $\text{K}_3[\text{Fe}(\text{CN})_6]$. Mol wt = 329.25 in order to obtain a final working solution of concentration 5 mg/ml of potassium hexacyanoferrate in 0.25 M sucrose solution.

Table 1. Treatment dosage (sub-lethal dose) based on the LD₅₀.

Group 1	Group 2	Group 3	Group 4	Group 5
LD50 for oral treatment of adult Wistar rats is K₃[Fe(CN)₆] 2,970 mg/kg BW (US, EPA 1990)				
20 mg/kg BW	12 mg/kg BW	6 mg/kg BW	2 mg/kg BW	0.25 M Sucrose

5 g of the CN salt was dissolved in 1000 ml of 0.25 M sucrose solution (β -D-Fructofuranosyl- α -D-Glycopyranoside; C₁₂H₂₂O₁₁; Mol. wt = 342.30; Sigma) (Varone et al., 2008).

Method of administration of cyanide solution

The animals were force fed orally using oral canula with a ball point at the tip. The animals were held with a glove with the left hand such that the neck region is held by the fingers to still the neck while being fed with the canula; treatment was done every morning before the animals were fed.

Grouping and treatment of animals

The treatment duration is 30 days: the total duration of the experiment is 80 days. The animals were kept under standard laboratory condition with alternating 12 h light and dark; they were fed on standard rat chow containing proteins, carbohydrate, fats, vitamins and minerals. Weight of the animals was measured at intervals of 3 days for the 30 days treatment duration Table 1 (Soler-Martin et al., 2010).

Sacrifice and specimen collection

The animals were sacrificed by cervical dislocation, the scalp was scraped and the skull immediately opened using a brain forceps, the skull was opened from the posterior part to leave the tissue intact (Van Zutphen et al., 1994). The V1 (primary visual cortex; designated as area 17 in the Brodmann's classification) was obtained from the rearmost portion of the occipital cortex, the superior colliculus was excised from the superior part of the copora quadrigemina, while the lateral geniculate body was traced to its sulcus at the base of occipital region. This was done for all the animals in each of the groups labelled Groups 1 to 5. The tissues were collected in specimen bottles containing the fixative "Formol Calcium".

Tissue processing for histology

Tissue processing for histology was done using the method of Pearse (1960) to obtain paraffin wax embedded sections; Fixation was done using formol calcium, dehydration in ascending grades of alcohol 50, 70, 90% and absolute alcohol I and II clearing- Xylene was used as the clearing agent (2 changes). Infiltration and embedding in paraffin wax (56°C Mpt) was done in the oven at 60°C, and the tissues were blocked out in paraffin wax.

Serial sections were obtained serially and the diameter varies for each of the histological method adopted for specific structure demonstration in the brain tissues.

Crystal violet for pyknotic nuclei

Paraffin wax sections about 8 μ m thick were used, the staining solution is prepared thus;

1. Crystal violet 1 g,
2. Distilled water 100 ml,
3. Acetic acid 0.25 ml.

The sections were taken to water (Pearse, 1960) and then stained in the cresyl fast violet staining solution for 25 min, they were rinsed in distilled water and allowed to stay in 96% alcohol until most of the stains has been removed (Um et al., 2010).

Gordon and sweet's method for silver impregnation of degenerating neurons

The following reagents were prepared:

1. Solution A: 2% silver nitrate,
2. Solution B: 2% potassium dichromate.

Tissue blocks were immersed in Solution B for 2 days, while dry tissue block with filter paper were immersed in Solution A for another 2 days, after which they were embedded in paraffin wax cutting sections (about 20 μ m thick), and then dehydrated, cleared and mounted (Guy et al., 2010).

Photomicrography and cell count

This was done using the LCD Bresser; cell count was done stereoscopically with the use Java application (Open Office Draw) with the magnification set at X400 on the Bresser, the image size and resolution remained unchanged and a line area was drawn on specific regions of the slide image (V1: Molecular layer, LGB: magnocellular layer and the SC: stratum superficiale). The magnification is a requirement for the cell count as the cell features and appearance were required in categorizing the cells as either apoptotic, normal or necrotic. The regions of the cell obtained were approximately predetermined; the orientation of the tissues prior to processing were similar and also serial sections were made and the third sections were considered for the cell count in all the slides used for this procedure.

RESULTS

Haematoxylin and eosin

The general morphology as demonstrated in Figure 1 (Hematoxylin and Eosin) shows the appearance of the molecular layer of the primary visual cortex (V1-Brodmann's Area 17), the distribution of the neurons, glial cells as well as projections to and from this layer of the neo-cortex. In the high dose treatment (20 mg/kg BW); the V1 shows a decrease in cell size for degenerating neurons 2.5 μ m Figure 1A (a) characterized by

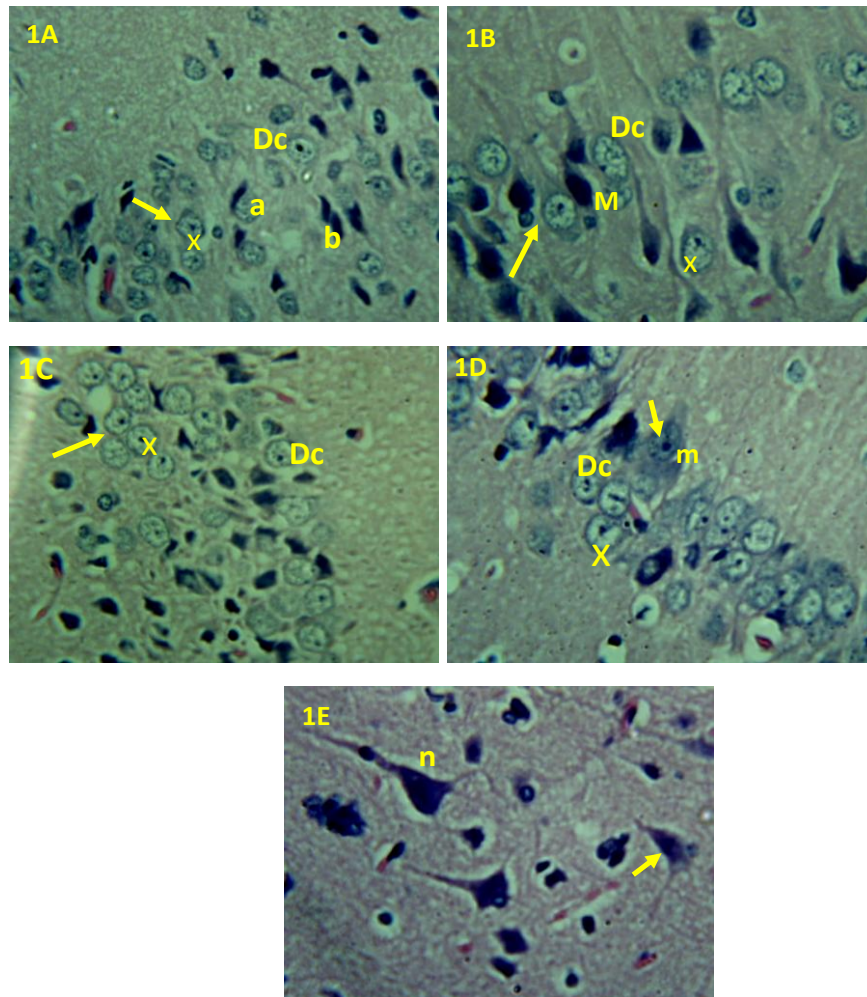


Figure 1A to E. H and E staining for general morphology of the primary visual area (V1) where A- Represents Group 1, B- 2.C- 3, D- 4 and E- 5. (M- molecular layer, X- degenerating cell, f- fibrous layer, Dc- degraded cytoplasm, N- normal cells). Arrow heads shows the relatively intact nature of the membrane and a centrally placed reduced nucleus (Magnification $\times 400$).

fragmented cytoplasm and a centrally placed darkly stained nuclei (Figure 1A -arrow head), loosely bounded fibrous axon (arrow head Figure 1B), smaller sized spiny neurons measures about $1.25 \mu\text{m}$ in diameter. The measurement was done stereoscopically at a magnification of $\times 400$ using a LCD Bresser microscope and analyzed on JAVA (Open office) platform. The control group consists of cells with darkly stained cell body resulting from hematoxylin staining of heterochromatin, the projections of the axons are prominent and the cytoplasm is not fragment as seen in the treatment group (Figure 1E). The cells do not show features of neuronal degeneration such as fragmented cytoplasm, loss of axons and loose fibres around a spherical cell body but rather possess a pyramidal cell body. The control group (Figure 1E) has a centrally placed nuclei measuring $0.6 \mu\text{m}$ in diameter compared with the single dot-like nuclei

in the degenerating cells of the treatment group (x) Figure 1A to D. The projections of the axons are prominent and the cell body are about $5 \mu\text{m}$ in diameter (Figure 1E) in the Group 1 (treatment group) the number of degenerating cells per/unit area (5 cm^2) is higher that the population observed in Group 2, such that in the highly dense region of group 1 (9 cells) (Figure 1A) while it is just about 3 cells over the same area in the highly dense region in Group 2 (Figure 1B), 7 in Group 3 (Figure 1C) and Group 4 (Figure 1D) has 8 cells [degenerating morphology based on parameters of Isom and Way (1999) could be described as apoptotic]. Although, the cell density per unit area is higher in Group 1, the diameter of the cell varies between the two groups with Group 2 cells measuring about $6 \mu\text{m}$ in diameter compared to the $2.5 \mu\text{m}$ observed in Group 1, Group 3 measures $5.6 \mu\text{m}$ while Group 4 measures about $5.1 \mu\text{m}$.

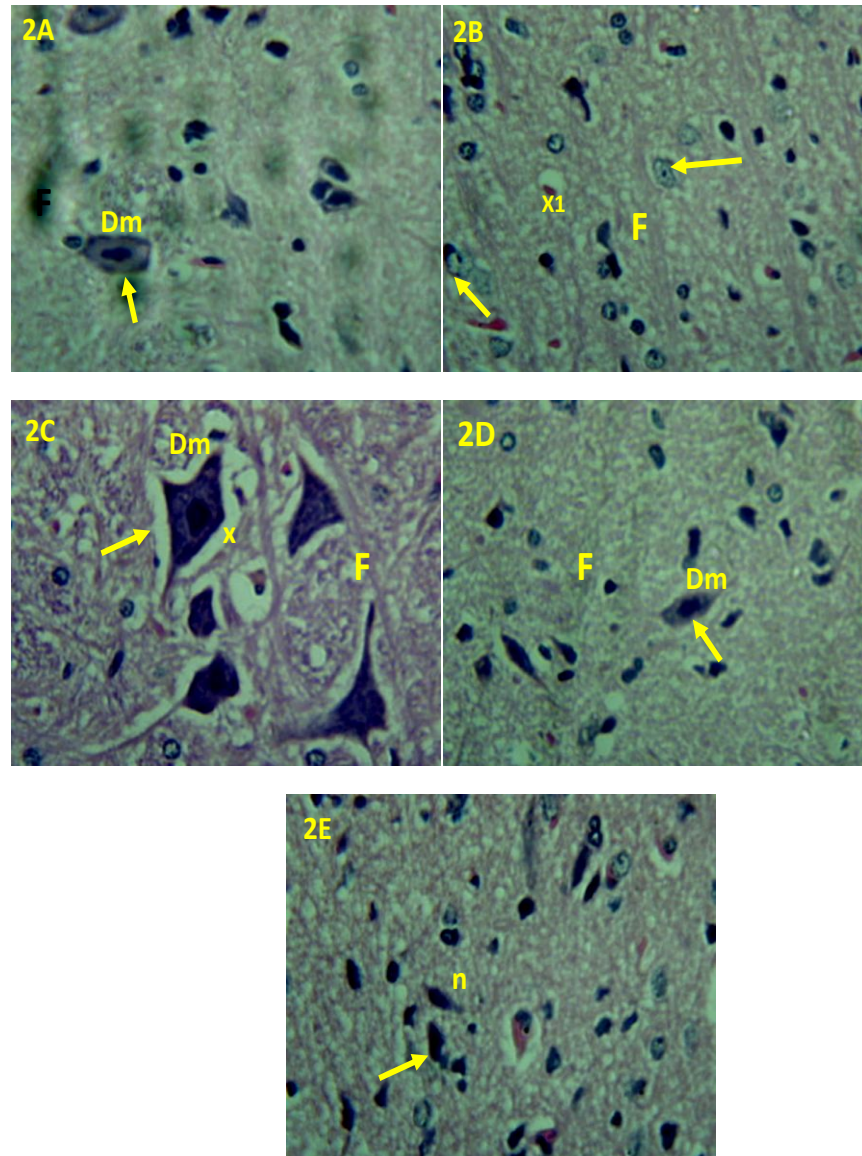


Figure 2A to E. H and E staining for general morphology of the LGB. Dm- degenerating membrane, f- fibrous layer, n- normal cells, x- vacuolar spaces) Arrow head shows thickened membrane measuring about 1.25 μm and giant nuclei of 2.5 μm in diameter (Magnification $\times 400$).

The extreme doses; the high dose treatment (20 mg/kg BW) and the low dose treatment group (2 mg/kg BW) recorded a close range in cell count based on the number of cells characterized by fragmented cytoplasm, loose fibres around cell body and shrunken nuclei.

In the lateral geniculate body (LGB), the high dose treatment group (Figure 2A) showed an increase in cell diameter of about 5 μm compared with the control group $\sim 1.25 \mu\text{m}$ (Figure 3E), the low dose treatment has a cell diameter close to that observed in the high dose treatment group which is about 4.5 μm , both of which are characterized by a dark stained shrunken nuclei of about 0.5 μm in diameter (Figure 2D). In the treatment Groups

1 and 4 (Figure 2A and D) loss of the fibrous layer was predominant while Groups 2 and 3 (Figure 2B and C) shows orientation of the fibrous layer with Group 2 (F) showing the highest cell density per unit area having degenerated cells (x) interspersed in between cells with normal morphology (x1) (Figure 2B). Group 3 (Figure 2C) shows the largest margin of increase in cell size with cells measuring about 6.25 μm and the nucleus is 1 μm in diameter, the thickness of the axon at the point of origin from the cell body is about 1.25 μm . In the LGB of the treatment group (Figure 2A to E) the predominant changes in the cells is characteristic cell enlargement (highest in Group 3, Figure 2C - 6.25 μm) as some of the

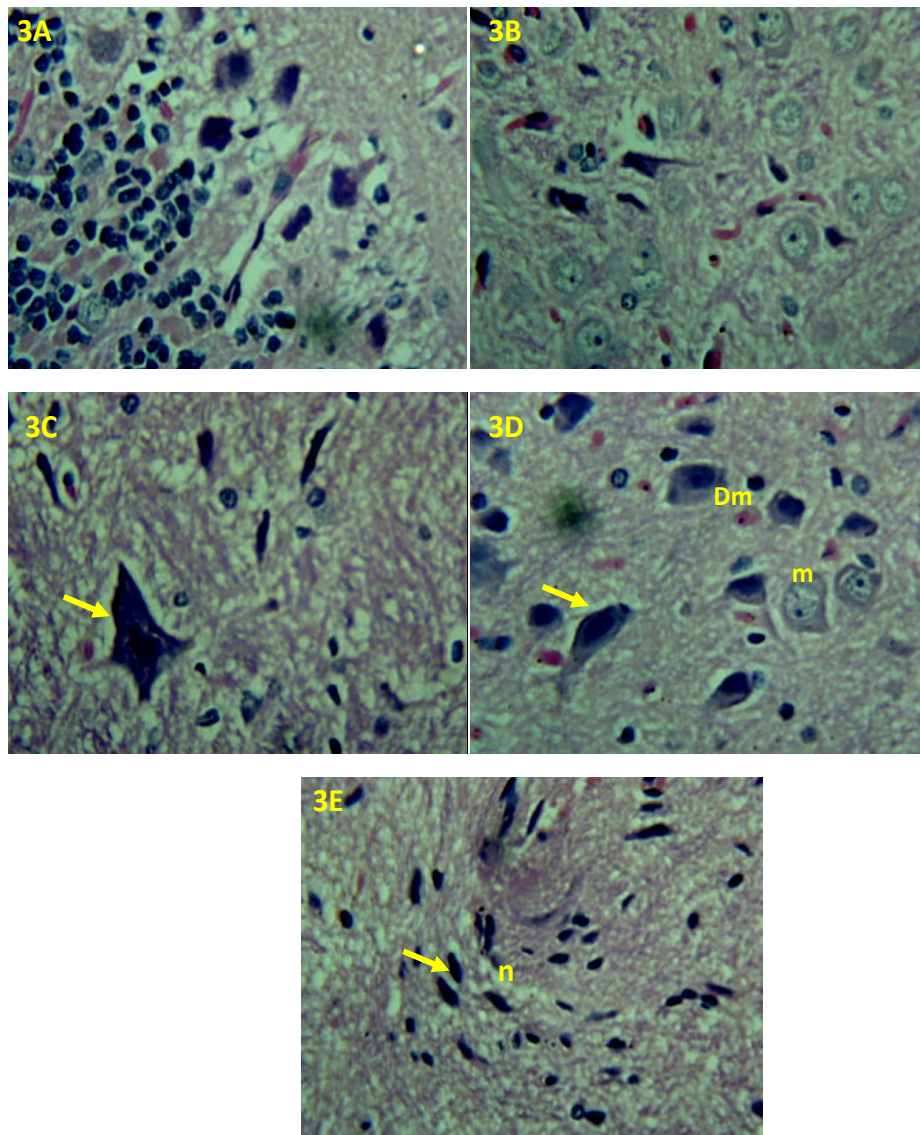


Figure 3A to E. H and E staining for general morphology of the superior colliculus. M- degenerating cells- n- normal cell, Dm- degenerating membrane, f- Fibrous layer, n- Normal cells, x- Vacuolar spaces). Arrow head shows thickened membrane measuring about 1.05 μm and giant nuclei of about 2.0 μm in diameter (Magnification $\times 400$). Haematoxylin and Eosin staining to demonstrate the general morphology of the treatment and control animals after 30 days of treatment (V1- H and E micrograph for the primary cortex, L1- lateral geniculate body and S1-superior colliculus).

cells shows loss of nuclei and thickening of the membrane or rather pronounced increase in cell diameter (Features of necrosis).

The cell distribution per unit area in the superior colliculus (SC) Group 1 (3 cells), 5 cells in Group 4, 6 cells in Group 4 and 12 cells in the control group, with the cells differing in morphology post-treatment, the cells shows fragmented cytoplasm and a pyknotic nuclei, in Group 1 LGB the membrane is highly distorted (y); characterized by thickening and retraction of the axonal projections from adjacent neuronal networks, some

points on the membrane appears invaginated. Group 3 (Figure 3C) arrow head shows enlarged cells measuring 6 μm also similar to the enlarged cell size observed in the LGB, also larger than the average cell enlargement observed in normal morphology cells of between 3.5 to 4 μm observed in (Groups 2, 3 and 4; Figure 3B, 3C and 3D), the nuclei are centrally placed and the number of degenerating cells is higher in Group 1, 2 and 4 which is about 3 cells (per 5 cm^2 at a magnification of $\times 400$). This is a silver iron-method for demonstration of cells with loss of cytoplasmic materials or rather fragmented

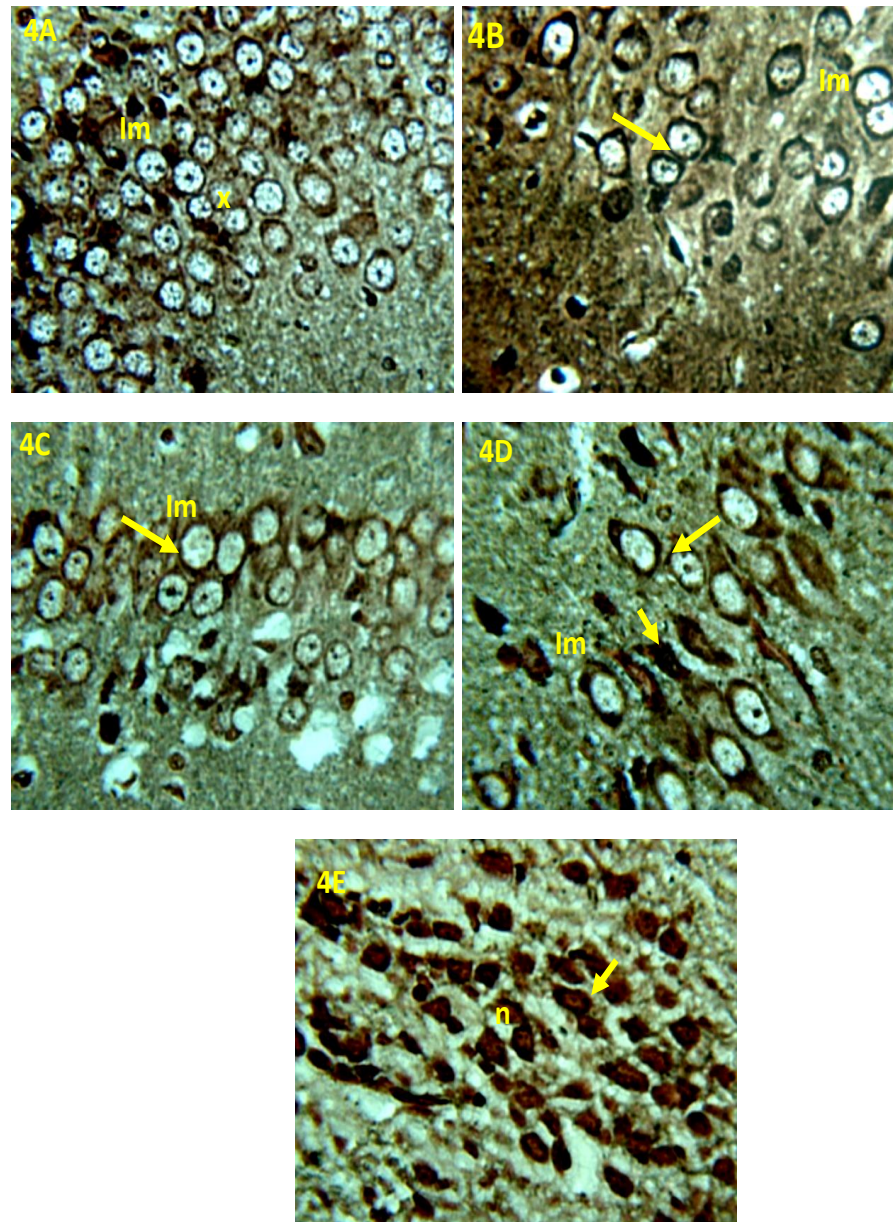


Figure 4A to E. Gordon and Sweet's silver-iron staining of the V1. (Im- intact membrane, x- cytoplasmic degeneration and vacuolar spaces. This is an indication of apoptosis in the V1 of the treatment groups (Figure 4A to D) Magnification $\times 400$.

cytoplasm (x) and degenerating axonal projections from the cells (a), this technique was used to support the observations from H and E for cells with degenerating cytoplasm as well as the distribution of these cells per unit area. The silver-iron method shows membrane integrity of the neurons and presence of reduced nuclei distinguishing it from cytoplasmic fragments observed in H and E and crystal violet, thus confirming the presence of a reduced nuclei in the treatment groups of the V1, in Figure 4A (High dose treatment group), the distribution of cells with unstained (Silver-iron negative), centrally or eccentric nuclei (Silver-iron positive) as well as intact

membrane suggests the cell are apoptotic. The neuronal projections are well defined in the 4th group (Figure 4D); on comparison with the high dose treatment Group 1 (Figure 4A) shows that although both have close cell diameter other structural differences exist between these two categories, which include presence of axonal projections in the low dose treatment group (arrow head Figure 4D) and total absence of such projections on Group 1, also the cell cluster observed in Group 1 was as a result of degenerated axonal projections thus causing the close approximation.

The degenerating fibrous layer of the SC and LGB

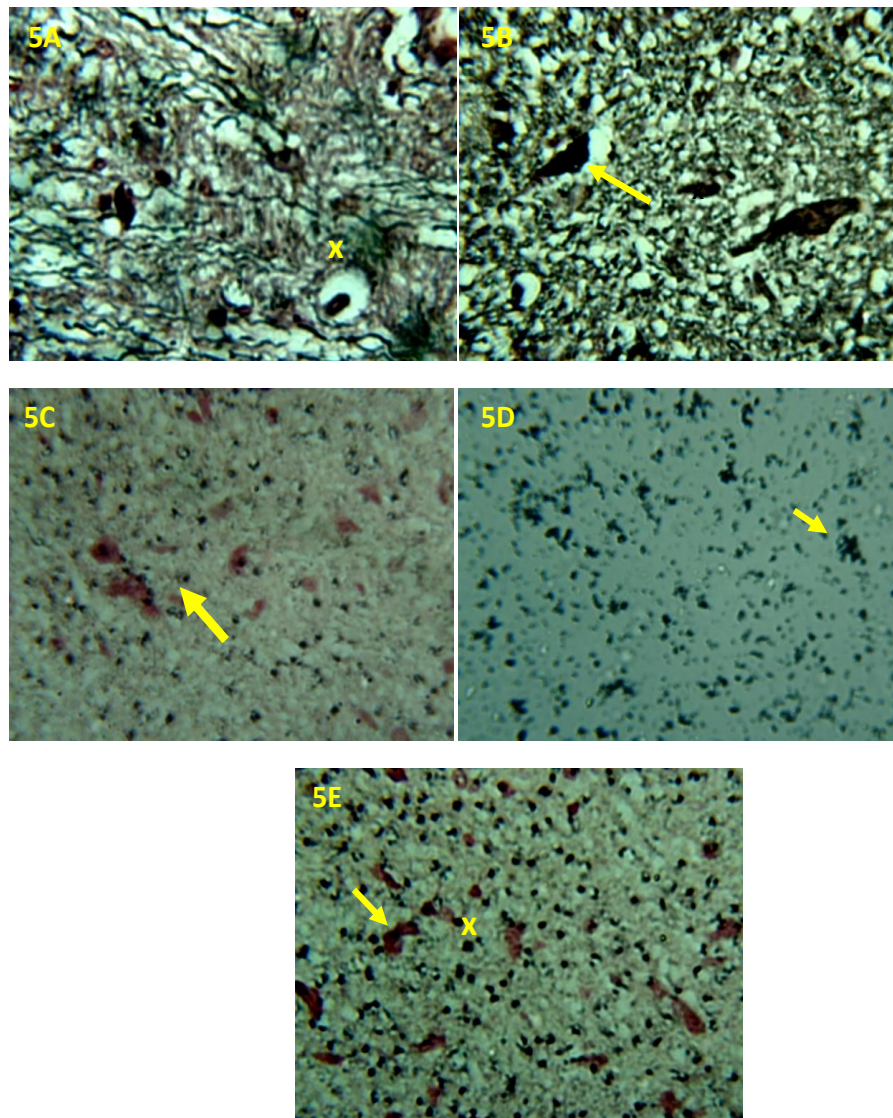


Figure 5A to E. Gordon and sweet's silver-iron staining of the LGB. Arrow head shows presence of degenerating membrane and no clearly bounded membrane structure, which suggests necrosis as the predominant cell death mode in this LGB (Magnification $\times 400$).

blobbed out to differentiate the fibrous layer (Arrow head) in the SC (Figure 5A to E). The degenerative features observed in the treatment group was absent in the control as the cytoplasmic content was stained rather than blank as seen in the treatment group (Figure 4A to D) compared with Figure 5E. Moreover, the Gordon and sweet's method for demonstration of neurodegeneration ($\times 400$) is shown in Figures 4 to 6.

Apoptosis; characterized by shrunken nuclei or pyknotic nuclei, fragmented cytoplasm, intact cell membrane is a predominant feature of cells in the V1 treatment group. Other parameters such as axonal projections, cell diameter and cell count per unit area vary with the treatment dose. Enlarged cell bodies features such as enlarged nuclei (prominent feature of

late stage necrosis), thickening of membrane, prolapsed membrane were the major observation in the LGB and SC also cell loss gave structures with predominant fibrous layers rather than an alternating cellular and fibrous layer in the laminae.

The Sc and LGB are laminated structures with alternating cellular and fibrous layers, it is observed that the fibrous layer is predominates in the treatment group as much as there is a reduction of the cellular layer, although certain number of cells are interspersed in between the fibrous layers some of these cells are characterized by enlarged cell body and nuclei, thickened cell membrane and loss of parts of the cell membrane (x) Figure 5A and B while necrotic sites with degenerating cells were observed in cells distributed in the fibrous

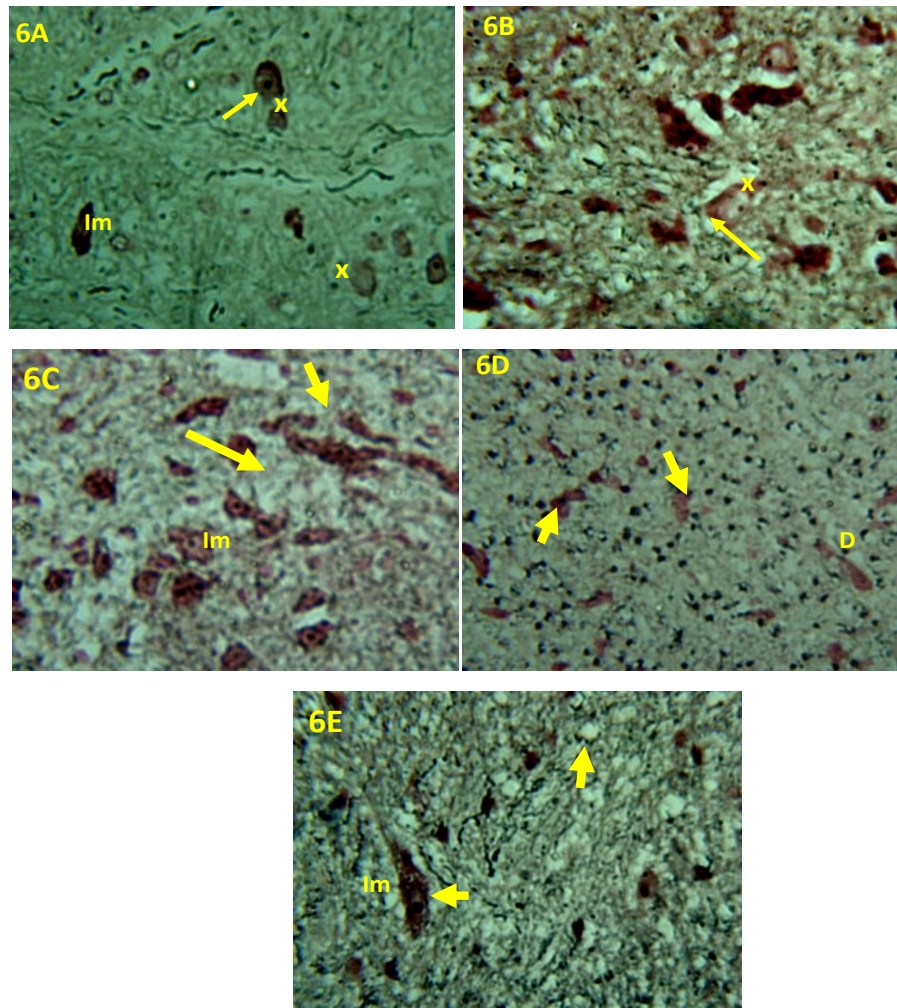


Figure 6 A to E. Gordon and Sweet's silver-iron staining of the SC. Dm- degenerating membrane, Im- intact membrane. Arrow head shows presence of degenerating membrane and no clearly bounded membrane structure, which suggests necrosis as the predominant cell death mode in this SC although apoptotic features was also observed (Magnification $\times 400$).

layer of the Groups 3 and 4 Sc (Figure 6C and D) arrow head.

Crystal violet

The cells in Group 3 (6 mg/kg BW/day) were observed in all the staining techniques employed to have undergone cell enlargement (Figures 7C, 8C and 9C). The treatment group shows loss of nissl substance in their cytoplasm (Arrow head), loss of nissl substance in the LGB was prominent in Groups 1 and 2 with loss of nissl substance in the cells of the V1 and relatively no loss in the SC (Figure 9A to E) arrow heads shows intense staining for nissl, although cell size is higher in cells with defective nissl substance (3.5 μm) compared to the 2.5 μm in the nissl stained cells as well as in the control group.

LGB: It was observed that nissl substance for enlarged cells were intensely stained with crystal violet (Figure 8A to E). Also, the fibrous layer is more prominent (f) with cells interspersed in the fibrous layer (arrow head Figure 8B and C). Some cells were also found to have apoptotic features such as fragmented cytoplasm, shrunk nuclei (y) in Figure 8C. The co-occurrence of apoptosis and necrosis in certain regions of the LGB and SC was demonstrated in the staining for nissl substance; Figure 9C (High dose treatment Group 1)- presence of necrotic tissue site (x) with prolapsed cell membrane and large eccentric and sometimes centrally placed nuclei with extracavations around degenerating cells. The cells in Group 3 (6 mg/kg BW/day) were observed in all the staining techniques. Crystal violet staining of the sections for V1, LGB and SC (Mag X400) are shown in Figures 7 to 9.

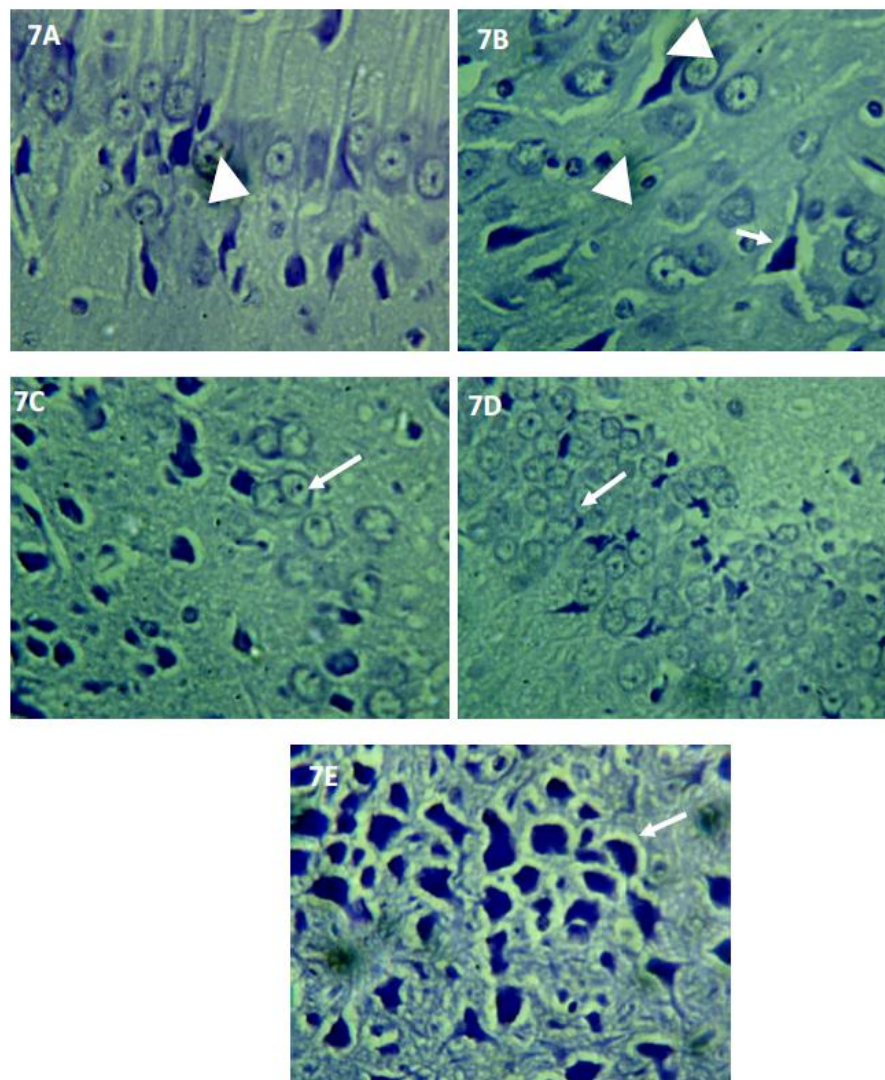


Figure 7A to E. Crystal violet (modified for nissl) for the V1 (Magnification $\times 400$).

In 14 N, arrow heads shows 3 adjacent cells a, b and c, where (a) is characterized by cell enlargement, knobbed axonal projection, (b) shows fragmented cytoplasm, pyknotic nuclei, intact cell membrane and (c) is a degenerated cell presumably in the advanced stage of necrosis characterized by small cell body and large space of about $3\ \mu\text{m}$ around the cell.

We determined the One-sample T test value for the normal cells and abnormal cells with either apoptotic or necrotic feature (Tables 3 and 4).

From graphical illustration the distribution of Φ in the Graph 1 shows that the number of normal looking cells was highest at the 6 mg/kg BW treatment group ($\Phi_{V1/Group\ 3}$) with an equilibrium almost attained in the rate of cellular degeneration at this treatment concentration ($\Psi_{V1/Group\ 3}$) in Graph 2. The highest normal cell distribution was observed in the control ($\Phi_{5.V1}$) as the least cell degeneration was found in $\Psi_{5.V1}$ also the control group.

Cell death was highest in $\Psi_{4.V1}$ which is the 2 mg/kg BW treatment group with most of the resultant cell death found to be mainly apoptotic on comparing the cell number per unit area. The distribution pattern in Φ_{LGB} was found to be similar to those observed in $\Phi_{.V1}$ and $\Phi_{.SC}$ with treatment, we found a closely related rate of cell survival in the LGB and SC, and this can also be correlated with the confidence interval values Table 3. Cell survival is highest at $\Phi_{5.SC}$ (control) while $\Phi_{2.SC}$ Table 4 has the highest survival rate among the treatment groups, $\Psi_{1.SC}$ recorded the highest number of degenerating cells per unit area with most of the degeneration found to be regional and characterized with vacuolar spaces around the cells; in the micrographs cell number per unit area was close to those of the control, special training techniques shows that most of this cells have characteristic loss of metachromasia and vacuolar spaces around these degenerating cells (necrosis). In the

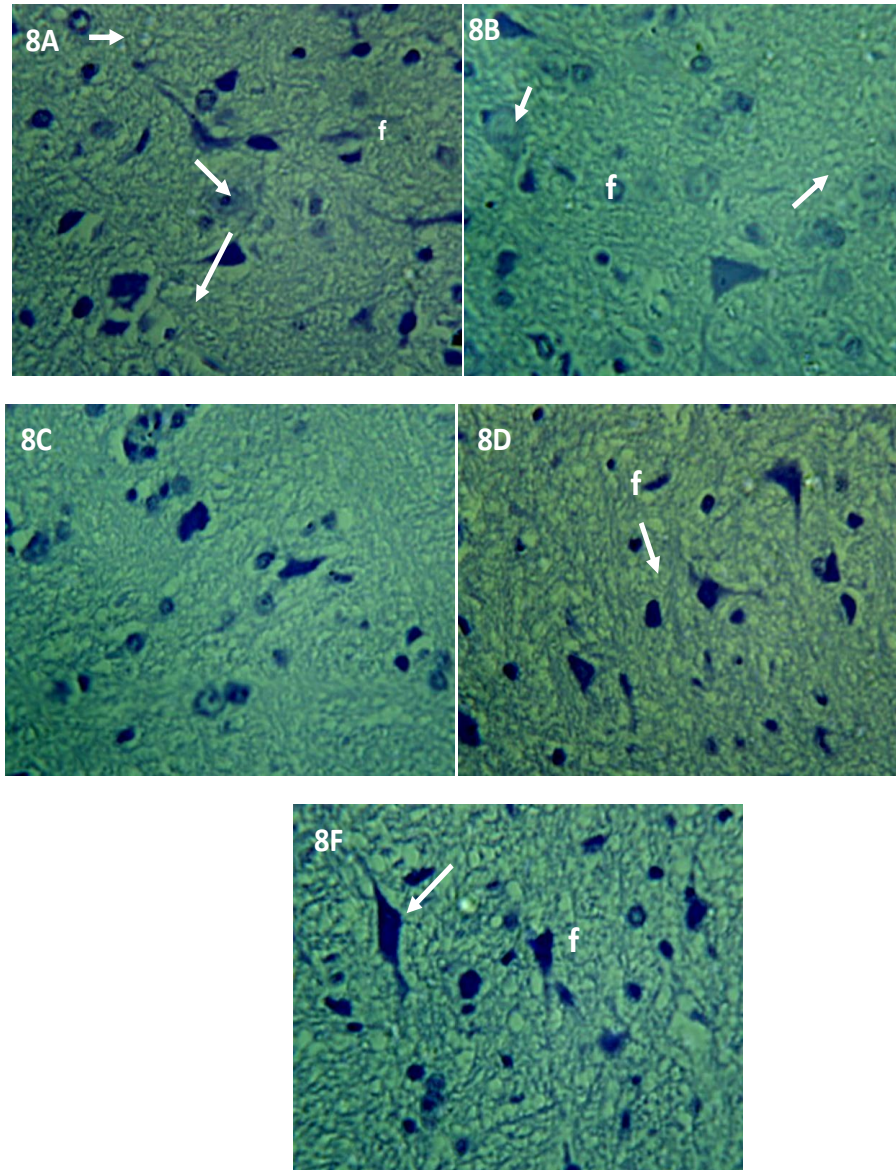


Figure 8A to E. Crystal violet (modified for nissl) for the LGB. f- Fibrous layer. Arrow head shows predominance of the fibrous layer of the LGB (Magnification $\times 400$).

V1 cells, degeneration was conserved to the cytoplasm while the cell sizes were increased considerably; similar changes were observed for the entire treatment group even though the number of cells per unit area differs considerably, with cell number greatly reduced in the high dose treatment group Table 2.

DISCUSSION

The present study uses chemical induction of cell death, to examine the morphology of neurons in the cerebral cortex (molecular layer) of rats, this was aimed at understanding the earlier findings involving the wide

distribution of movement disorder and loss of vision in cassava endemic regions of Tanzania, Mozambique, Niger and Nigeria (Osuntokun et al., 1981), for cell death analysis we choose crystal violet staining for fragmented nuclei and nissl (Sharma and Chalam, 2009), Gordon and sweet silver-iron staining for degenerating neurons (Guy et al., 2010), Hematoxylin and eosin to demonstrate cell morphology and immuno staining to demonstrate T-cell infiltration of cell death sites (apoptosis or necrosis). These complimentary and independent methods all demonstrated a large increase in cell death in the V1, LGB and SC of rat models treated with potassium hexacyanoferrate to mimic movement disorders and loss of vision associated cassava endemicity and

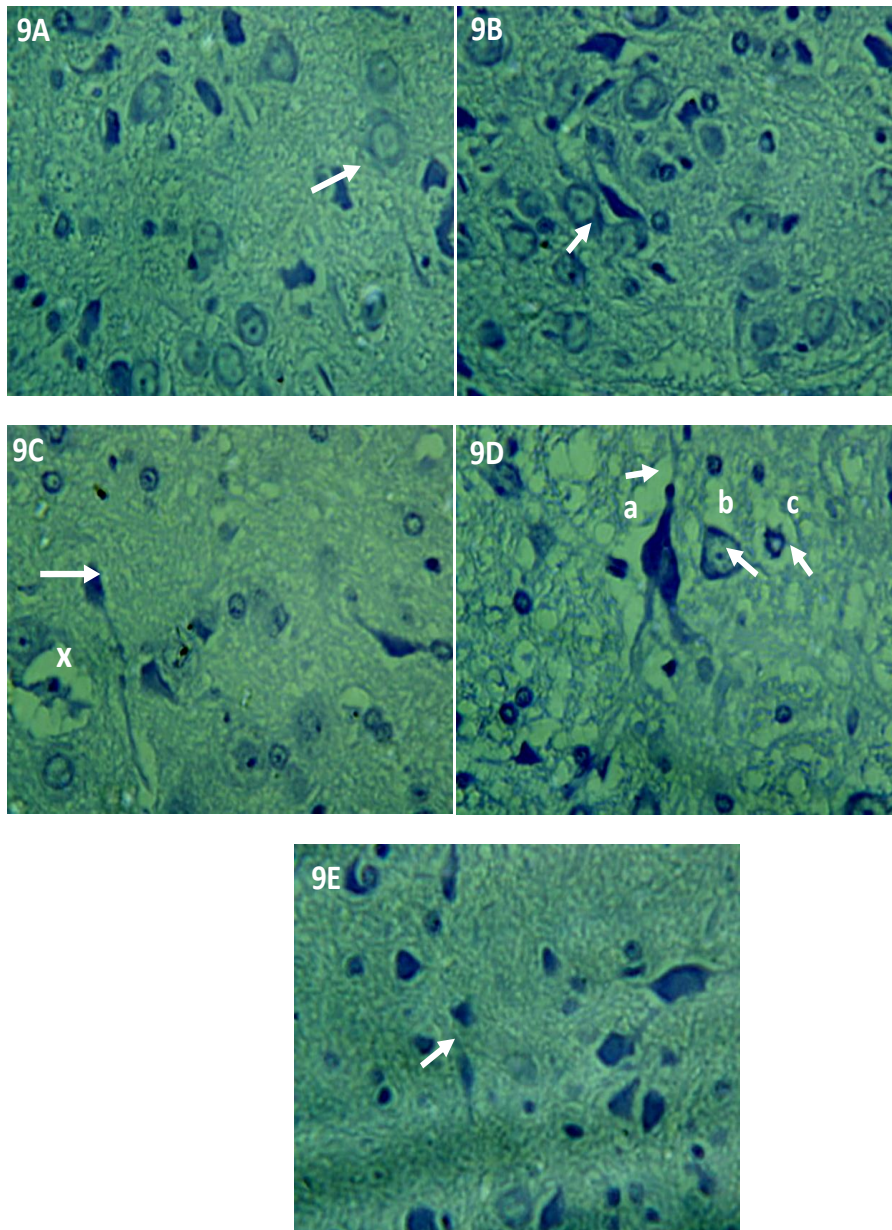
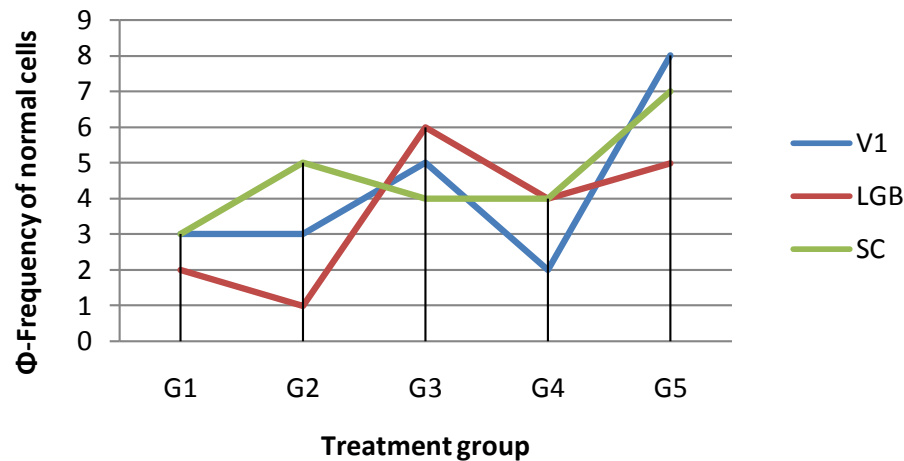


Figure 9A to E. Crystal violet (modified for nissl) for the SC. X- Degenerated cell, a- enlarged cell with prominent projections, b- characteristic apoptosis, c- characteristic necrosis (Magnification x400).

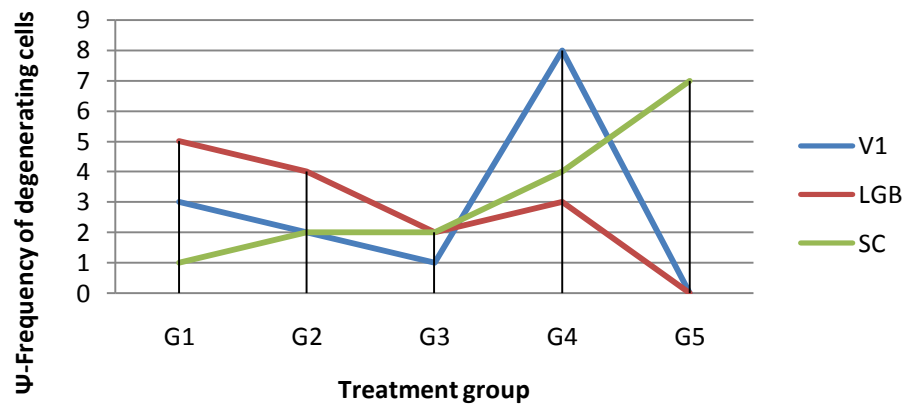
consumption (note that cassava also contains scopoletin and aflatoxin which are known neurotoxins). Although none of this method is specific for any particular neuron type, the advantages of using these five methods together are as follows: (1) H and E staining reveals cell morphology to include nuclei, nissl and membrane as well as extents of neuronal connections and necrotic sites at higher magnifications; (2) Analysis of pyknotic nuclei using nissl staining allows on the same section both a quantitative measurement of cell death and a direct evaluation of anatomical parameters for example, (the area of the V1); (3) Silver-iron staining method

demonstrates agyrophylic extracellular materials, degenerating neuronal membrane and loss of cytoplasmic materials.

Cellular composition has impact on how the cell moderates its demise or rather the pattern of cell death adopted by the cells in excitotoxicity (like those observed in cyanide intoxication), Previous studies we conducted on the phosphatase system showed that increased lysosomal activity by a measure of acid phosphatase (ACP) was associated with rapidly degenerating cytoplasm at high magnifications while necrotic sites and disruption of membrane structure was found to correlate



Graph 1. Φ -distribution of normal cells in the treatment groups and the control.



Graph 2. Ψ -Distribution of degenerating cells in the treatment and the control group.

with drastic rise of alkaline phosphatase activity (ALP) at first followed by a steep drop. Other experiments by Jensen et al. (1999) has shown that deletion of NMDA R1 receptors in mice rescues developing cerebellar granule cells, presumably due to excitotoxicity, and a link has been found between cyanide and NMDA receptors; cyanide is capable of potentiating NMDA receptors thus allowing the cell to be prone to excitotoxicity, this could also be attributed to the rather large sizes of the neurons although the neuronal size did not follow a regular pattern. Aside increase in cell death, there was also a reduction in cell number per unit area in the V1, LGB and SC with the highest effect found in V1 for the treatment groups when they were compared with the control, an early increase in size followed a great size reduction in certain cells may be explained by prolonged use "Excitability" followed by peaked oxidative stress, then a loss of cytoskeleton and membrane which might account for the reduced cell size and the presence of necrotic sites around this regions and were observed to have lost

neuronal connections. However, overlap of cell death with synapse loss in necrosis raises important issues as this differ from the observations in apoptosis where neuronal connection was relatively unchanged it is possible that defective membrane observed in necrosis causes defective synaptic connection then increased cell death it will be important to investigate actin nucleation assembly in dendritic branching of wild type (WT) and WT models treated with K-hexacyanoferrate Table 5.

Necrosis is accompanied by inflammatory infiltrate phagocytic cells. DNA degradation, if it occurs, is a late event (Katherine et al., 2001), In the LGB Figure 2C and the SC (Figure 3C) were found to have enlarged cells of about 6.1 μm in diameter and giant nucleus reaching about 1 μm in length, It was also observed that the adopted mode of cell death is dose dependent such as that which was observed in the treatment Group 3 (6 mg/kg BW) was found to have characteristics of necrotic cells in the LGB and SC (Figure 2C and 3C), the high dose treatment (20 mg/kg BW) and the low dose

Table 2. Cell count.

Group	V1		LGB		SC	
	Φv	Ψv	ΦL	ΨL	Φs	Ψs
1	3	3	2	5	3	1
2	3	2	1	4	5	2
3	5	1	6	2	4	2
4	2	8	4	3	4	4
5	8	0	5	0	7	0

Ψ represents the number of cells having a normal appearance, Φ represents the number of cells having necrotic appearance, which includes vacuolar spaces around the cell, loss of neuronal connection and damaged membrane while features of apoptosis (Pyknotic nuclear, reduced Metachromasia of the membrane and relatively intact cell membrane on comparison with the normal.

Table 3. Descriptive statistics for the number of normal cells observed.

Parameter	N	Minimum	Maximum	Mean	Std. Deviation
V1	5	2.00	8.00	4.2000	2.38747
LGB	5	1.00	6.00	3.6000	2.07364
SC	5	3.00	7.00	4.6000	1.51658
Valid N (listwise)	5				

Table 4. Descriptive statistics for number of cells found undergoing either apoptosis or necrosis

Parameter	N	Minimum	Maximum	Mean	Std. Deviation
V2	5	0.00	8.00	2.8000	3.11448
LG2	5	0.00	5.00	2.8000	1.92354
SC2	5	0.00	4.00	1.8000	1.48324
Valid N (listwise)	5				

V1- normal cells in the visual cortex, while V2 represents damaged cells found to have one or more features of neurodegeneration, LG2- cells undergoing degeneration in the lateral geniculate body and SC2- degenerating neurons of the superior colliculus.

Table 5. Table showing distribution of mode of cell death in the V1, LGB and SC.

Parameter	Group 1	Group 2	Group 3	Group 4	Group 5
V1	Apoptosis	Apoptosis with partial necrosis	Apoptosis	Apoptosis	Normal
LGB	Necrosis	Necrosis/Apoptosis	Necrosis	Necrosis	Normal
SC	Necrosis	Necrosis/Apoptosis	Necrosis	Apoptosis/Necrosis	Normal

treatment (2 mg/kg BW) were seen at certain instances to elicit similar changes in cell morphology, in the V1 (1A and 1D) cell diameter was 5.0 and 5.1 μm , respectively with both having features like fragmented cytoplasm, loose fibres around the cell body, centrally placed shrunken nuclei and intact cell membrane (apoptosis) also the cell count per unit area was 8 and 9 respectively Table 2, another finding to support this hypothesis is in the LGB where the cell diameter in Group 1 is 4.4 μm in Group 1 and 4.5 μm in Group 4 with both having enlarged nuclei measuring 0.5 μm , as a matter of general

observation the fibrous layer was predominant in LGB of both groups. The question about the similarity in features induced at these two treatment dosages is that, is the rate of progression of these features at the same rate?, the answer to this was indirectly invested by the DAB immunostaining for light chains immunoglobulin turned out to show that even though generally morphology suggests similar changes, IgG studies show that both are in different stages of the cell change, while immuno studies revealed it. The loose fibres counterstained around the cell bodies of the Group 4 treatment group are entirely

absent in Group 1, thus implying loss of counter stain of axonal projections. Although, these projections were observed in H and E, crystal violet (CV) and Gordon and sweet's method, it is observed that protein turnover required to detect this projections were relatively absent in Group 1 at this stage but still present in Group 4, likewise the intensity of the DAB-PAP silvers intensification was found to be of higher intensity in the Group 1 with most of the activity covering the membrane and cytoplasmic area and lower intensity in the Group 4 with most of the activity restricted to the membrane area, the predominating fibrous layers in the LGB and SC of Groups 3 and 4 was shown by intense brown deposits of fibers interlaced around the cells. Aside dose dependence in adopted mode of cell death it also varies for different parts of the brain with apoptosis predominant in the visual cortex and necrosis in the LGB and SC although certain level of occurrence of apoptosis may be found in the LGB and SC. This could explain the variation in region specific cytotoxic pathways observed in the different parts of the brain.

Conclusions

Cyanogenic neurotoxicity involves chemical induction of cell death; the adopted mode of cell death was found to be dose dependent in a particular region of the visual relay centre, and also will vary for the various V1, LGB and SC for the same treatment dose, this however, supports the fact that the different regions of the visual cortex has different cytotoxic pathway and the mode of cell death will depend on how the region respond to the assault. The predominant mode of cell death in the V1 is apoptosis while necrotic tissue sites were found to exist in the SC of the same treatment, certain cells in the LGB showed morphological features of both apoptosis and necrosis. The extreme doses gave similar events in terms of cell morphology and count per unit area.

ACKNOWLEDGEMENTS

The authors are grateful to the West African Health Organization; Trinitron Biotech Ltd; University of Ilorin; Departments of Anatomy and Histopathology, National Hospital, Abuja, Nigeria; and to Pharm. Mike Omotosho.

REFERENCES

- Almer M, Van der S, Nelson L (2006). Acute cyanide toxicity: mechanisms and manifestations. *J. Emerg. Nurs.*, Aug; 32(4 Suppl): S8-11.
- Behar TN, Scott CA, Greene CL, Wen X, Smith SY, Maric D, Liu QY, Colton CA, Barker JL (1999). Glutamate acting at NMDA receptors stimulates embryonic cortical neuronal migration. *J. Neurosci.*, 19: 4449-4461.
- Bhattacharya R, Tulsawani R (2008). *In vitro* and *in vivo* evaluation of various carbonyl compounds against cyanide toxicity with particular reference to alpha-ketoglutaric acid. *Drug Chem. Toxicol.*, 31(1): 149-61.
- Bhattacharya R, Lakshmana RPV (2001). Pharmacological interventions of cyanide-induced cytotoxicity and DNA damage in isolated rat thymocytes and their protective efficacy *in vivo*. *Toxicol. Lett.*, 119: 59-70.
- Bonfoco E, Krainc D, Ankarcona M, Nicotera P, Lipton SA (1995). Apoptosis and necrosis: Two distinct events induced respectively by mild and intense insults with NMDA or nitric oxide/superoxide in control cell cultures. *Proc. Natl. Acad. Sci. USA.*, 92: 7162-7166.
- de Haro L (2009). Disulfiram-like syndrome after hydrogen cyanamide professional skin exposure: two case reports in France. *J. Agromedicine*, 14(3): 382-384.
- de la Cruz Cosme C, Medialdea Natera P, Romero Acebal M (2009). Amyotrophic lateral sclerosis syndrome-plus and consumption of cassava (Manihot). Is this a new presentation of the neurotoxic motor-neuron syndrome? *Neurologia*. 2009 Jun, 24(5): 342-343.
- Gamper N, Li Y, Shapiro MS (May 18 Epub 2005). Structural requirements for differential sensitivity of KCNQ K⁺ channels to modulation by Ca²⁺/calmodulin. *Mol. Biol. Cell*, 8: 3538-51.
- Gilman S, Koeppe RA, Nan B, Wang CN, Wang X, Junck L, Chervin RD, Consens F, Bhaumik A (2010). Cerebral cortical and subcortical cholinergic deficits in Parkinsonian syndromes. *Neurology*. 2010 May 4, 74(18): 1416-1423.
- Guy S, Catherine T, Xiao-Qing T, Sara W, Feng Z, Xiaodong L, Poonit K, Goran P, Tanya D, Antoniette J, Paul B, Nicole B, Grant ED, Mark Z, Donald SK (2010). Positive allosteric modulators of the human sweet taste receptor enhance sweet taste PNAS 2010, 107(10): 4746-4751.
- Guy S, Catherine T, Xiao-Qing T, Sara W, Feng Z, Xiaodong L, Poonit K, Goran P, Tanya D, Antoniette J, Paul B, Nicole B, Grant ED, Mark Z, Donald SK (2010). Positive allosteric modulators of the human sweet taste receptor enhance sweet taste PNAS 2010, 107(10): 4746-4751.
- Isom GE, Gunasekar PG, Borowitz JL (1999). Cyanide and neurodegenerative disease. In *Chemicals and Neurodegenerative Disease* (Bondy SC, Ed.), Prominent Press, Scottsdale, AZ, pp. 101-129.
- Jensen P, Surmeier DJ, Goldowitz D (1999). Rescue of cerebellar granule cells from death in weaver NR1 double mutants. *J. Neurosci.*, 19: 7991-7998.
- Katherine L, Barrett JM, Willingham A, Julian G, Mark CW (2001). Advances in cytochemical apoptosis. *J. Histochem. Cytochem.*, 49: 821-832.
- Lee B, Park J, Kwon S, Park MW, Oh SM, Yeom MJ, Shim I, Lee HJ, Hahn DH (2010). Effect of wild ginseng on scopolamine-induced acetylcholine depletion in the rat hippocampus. *J. Pharm. Pharmacol.*, 62(2): 263-271.
- Li R, Sonik A, Stindl R, Rasnick D, Duesberg P (2000). Aneuploidy vs. gene mutation hypothesis of cancer: Recent study claims mutation but is found to support aneuploidy. *Proc. Natl. Acad. Sci. USA*, 97: 3236-3241.
- Mathangi DC, Namasivayam A (2000). Neurochemical and behavioural correlates in cassava-induced neurotoxicity in rats. *Neurotox. Res.*, 2(1): 29-35.
- Osuntokun BO (1981). Cassava diet, chronic cyanide intoxication and neuropathy in Nigerian Africans. *World Rev. Nutr. Diet*, 36: 141-173.
- Pearse AGE (1960). *Histochemistry*. Little, Brown and Company. Boston 1960.
- Pedro RN, Thekke-Adiyat T, Goel R, Shenoj M, Slaton J, Schmechel S, Bischof J, Anderson JK (2010). Use of Tumor Necrosis Factor-Alpha-coated Gold Nanoparticles to Enhance Radiofrequency Ablation in a Translational Model of Renal Tumors. *Urology*. 2010 May 6 (Ahead of Print).
- Prabhakaran K, Li L, Zhang L, Borowitz JL, Isom GE (2007). Upregulation of BNIP3 and translocation to mitochondria mediates cyanide-induced apoptosis in cortical cells. *Neuroscience*, 150(1): 159-167.
- Quintavalle C, Incoronato M, Puca L, Acunzo M, Zanca C, Romano G, Garofalo M, Iaboni M, Croce CM, Condorelli (2010). G. activity. *Cell Death Differ.*, 2010 May 28.
- Sharma RK, Chalam KV (2009). *In vitro* evaluation of bevacizumab toxicity on a retinal ganglion cell line. *Acta Ophthalmol.*, 87(6): 618-22.

- Soler-Martín C, Riera J, Seoane A, Cutillas B, Ambrosio S, Boadas-Vaello P, Llorens J (2010). The targets of acetone cyanohydrin neurotoxicity in the rat are not the ones expected in an animal model of konzo. *Neurotoxicol. Teratol.*, 32(2): 289-294.
- Svendsen P, Hau J (eds.) (1994). *Handbook of Laboratory Animal Science*, volume I, Selection and handling of animals in biomedical research. CRC Press.
- Um YJ, Jung UW, Kim CS, Bak EJ, Cha JH, Yoo YJ, Choi SH (2010). The influence of diabetes mellitus on periodontal tissues: A pilot study. *J. Periodontal Implant Sci.*, 40(2): 49-55.
- Van Zutphen LFM, Baumans V, Beynen AC (1994). *Principles of Laboratory Animal Science*. Elsevier.
- Varone JC, Warren TN, Jutras K, Molis J, Dorsey J (2008). Report of the investigation committee into the cyanide poisonings of Providence firefighters. *New Solut.*, 18(1): 87-101.
- Varone JC, Warren TN, Jutras K, Molis J, Dorsey J (2008). Report of the investigation committee into the cyanide poisonings of Providence firefighters. *New Solut.*, 18(1): 87-101.
- Vicente T, Eva S, Margaret MM, Robbert HC, Afshin S, Luis S, Wim JQ (2006). Designed tumor necrosis factor-related apoptosis-inducing ligand variants initiating apoptosis exclusively via the DR5 receptor. *Proc. Natl. Acad. Sci.*, 103(23): 8634-8639.